SHAPE OPTIMIZATION OF A CAST TURBINE MANIFOLD

BY

W.A. Holzmann
GenCorp Corporation, Aerojet Propulsion Division

&

V.J. Wagner
The MacNeal-Schwendler Corporation

ABSTRACT

This paper discusses the application and lessons learned using the Shape Optimization capabilities in MSC/NASTRAN to analytically modify the existing design of a cast turbine manifold. Figure 1 shows a model of a typical cross section of the manifold. The objective of the analysis was to minimize weight while satisfying several load conditions as well as manufacturing and assembly constraints. Using MSC/PATRAN, a solid finite element wedge model of the cross section of the manifold was created. Basis vectors were generated with the analytical boundary method and used as shape design variables. The approach and results are discussed, as well as recommendations for future production use of the optimization capability.

INTRODUCTION

The objective of this work was to redesign an existing turbine manifold of a rocket engine to minimize weight (cross section, Figure 1). As with all space boost vehicles, weight minimization is of primary importance since this translates directly to increased payload. To control the direction of the allowable shape changes in the manifold casting, the analytical boundary method approach in MSC/NASTRAN was used for defining the basis vectors. The basis vectors are user defined permissible displacement fields that, as part of the optimization process, are scaled and linearly combined to determine the allowable move directions of the finite element (FE) grids. The scaling terms applied are referred to as design variables, and are calculated based on the sensitivities of the design objective (weight).

For this application, the final optimization solution used three basis vectors which controlled the contour of the manifold's outer surface. The current method of selecting basis vectors can be improved based on the user's experience and judgment, and requires a comprehensive set of move vectors capable of capturing the true optimal shape. The majority of the total analysis time was spent determining an acceptable set of allowed shapes. Four complete design iterations, with differing basis vectors, were performed before the final set of basis vectors was selected.

PROBLEM DEFINITION

Due to the complexity of the manifold system and constraints, a systematic, computer based method for identifying potential design improvements was required. As the manifold is a solid, cast component, MSC/NASTRAN's shape optimization capability was identified as a potential solution to modify the cast shape to meet weight objectives and design constraints within a limited schedule and Engineering budget. The method significantly increased the effectiveness of the analysis for determining and recommending design modifications compared to traditional trial and error approaches.

Design constraints were identified based on system and manufacturing requirements. In terms of engine system performance, limits were required for deflections on the stator vane ends (Figure 2). Large stator vane distortions and nozzle area variations would result without these displacement limits, resulting in combustion inefficiency. All relative displacement constraint limits specified were based on post-fire rub block data from full engine system level tests.

Manufacturing constraints, which were introduced mid-program, were based on input from the casting vendor. Practical design limits were needed for manifold wall thickness and tapers in order to insure an acceptable and reproducible casting based on minimum void and material grain size requirements. (Figure 2). Finally, component peak stress limits were imposed on the entire manifold based on the Von-Mises yield criteria.

ANALYSIS SETUP

As part of a preliminary stress analysis of the complete turbine manifold assembly, a non-linear 2-D axisymmetric analysis was performed. The objective of the analysis effort was to minimize the weight of the assembly by reducing the mass of the primary manifold. The assembly model included nonlinear gap elements to represent the contact surfaces between the manifold and the remainder of the turbopump assembly (TPA).

The applied loads to the system included thermal profiles from the system MSC/PThermal model, and thrust point loads. Static nonlinear solutions at selected time slices in the transient were made to identify the most severe loading condition based on manifold stress predictions. The manifold boundary conditions in the TPA for displacement, temperature, pressure, and forces corresponding to these maximum stresses were then used as static inputs to the optimization model.

As the MSC/NASTRAN shape optimization solver does not apply to axisymmetric models, a solid three dimensional sector of the turbine manifold was created. The planar geometry of the manifold cross section was imported from Pro/E. Only the turbine manifold portion of the assembly was included in the

shape optimization model since it was the component selected for redesign. This also greatly reduced the size of the problem and eliminated the gap elements used to represent contact surfaces.

The FE model (Figure 1) was created by importing the quad shell elements from the axisymmetric 2-D analysis, then extruding a single layer of solid CHEX8 elements by rotating the quads about the TPA centerline. Using the same mesh as the 2-D analysis allowed correlation between the axisymmetric and the solid analyses. In addition, this also provided identical grid points for application of the manifold loads and boundary conditions predicted by the system analysis.

The model consisted of 2397 grids and 1071 CHEXA8 solid elements. In order to keep the side or cut surfaces in-plane, a local cylindrical coordinate system was created so that the hoop direction degrees of freedom could be constrained.

The initial conditions of the model used in the optimization process included the thermal profile from PThermal, displacements and forces at the cut boundaries, and internal pressures due to fuel flow. Figure 3 shows the thermal contours and Figure 4 illustrates the defined pressure profiles and loads.

DESIGN MODEL SETUP AND EVOLUTION

The MSC/NASTRAN optimization solution 200 was used for this analysis. Of the four possible methods for basis vector generation, the analytical boundary shape method was selected due to its relative generality. In addition, this method also updates the basis vectors after every design cycle, hence reducing mesh distortion problems associated with large shape changes, which appeared likely at the onset of the analysis.

The objective for the analysis was to minimize the weight of the solid manifold. Initial constraints were based both on Von Mises stress using the DRESP1 entry, and performance related displacements using DRESP1 and DRESP2 with DEQATN entries. As predicted in the nonlinear system model, a local area of analytically high predicted stress induced by incorrect geometry was verified. Because the product team was able to determine several simple design modifications to reduce the stress in this region, it was excluded from the stress constraint by omitting the property ID from the DRESP1 entry for the design model.

Upon completion of the basic analysis, design, and auxiliary models, a series of optimization passes were made. Each analysis used a different set of basis vectors as results and design information became available.

A significant amount of time was spent generating a set of acceptable basis vectors to direct the shape changes of the manifold. The basis vectors were generated by use of the auxiliary 'skin' model of shells on the exterior surface of the manifold solid model. A series of static solutions were made for various load and boundary conditions applied to the submodel of CQUAD4's. After reviewing the distorted shapes from the static runs, a set of candidate vectors was determined.

The first optimization analysis used eight basis vectors created using PLOAD4 surface pressures on the shell elements. The pressure distributions were specified using field definitions associated with geometric surface entities in MSC/P3. As is evident from Figure 5, the analytical shape change achieved by this optimization pass was unacceptable. Hard convergence was not achieved due to a violation of the thickness constraints.

The second optimization analysis was performed by manipulation of the linear scaling factors of the basis vectors via the DVBSHAP entry. Experimentation was also made with the initial values of the design variables as well as the fractional change move limits on the DESVAR entry. This produced a more acceptable manifold shape change, but convergence was still not achieved. (See Figure 5).

Prior to the third optimization pass, detailed wall thickness and taper requirements were obtained from the manifold casting manufacturer (see Figure 2). This information was then included in the manifold

thickness constraints. The basis vector controlling the shape of the flat surfaces of the manifolds was also modified. This was accomplished using SPCD enforced displacements on the auxiliary model grids rather than defining pressure loads on the shells. This method provided significantly greater shape control of the basis vector and insured that the resulting shape of the manifold would have flat surfaces for this region. Figure 5 shows that the manifold shape improved after the third attempt in terms of material reduction while maintaining reasonable flat surfaces for the casting. Unfortunately, the toroidal thin walled areas assumed a 'lobed' appearance due to insufficient control of the basis vector in this region.

The casting part thickness and taper requirements were constrained using DRESP2 entries with associated equations defined on the DEQATN entry. The constraint equation was used to control the relative motion between selected grids specified by the DNODE field on the DRESP2 entry. Due to the limitation of the DNODE referencing only global Cartesian degrees of freedom, the manifold model was positioned so that the center of the toroidal section was on the global origin. This allowed the radial wall thickness to be calculated by root summing the square of the global x and y displacements of the selected grids.

The final optimization analysis was made by redefining the basis vectors associated with the thin wall section. Two additional basis vectors were created using SPCD enforced displacements on the surface grids. The three basis vectors for the final analysis are shown in Figure 6, and the final shape is shown in Figure 5.

OPTIMIZER RESULTS

As shown in Figure 7, the optimizer was allowed to perform 28 design iterations. This relatively large number was allowed due to the small size of the model (fast turnaround) and the progression of the objective function. Total cpu time for all 28 cycles was 2650 seconds on a Sun Sparc 20, with a maximum used memory (Hiwater) of 3.86 MWords.

For this analysis, hard convergence was not achieved based on the default convergence criteria, meaning that the final results represented an infeasible design. For the 28th cycle, the relative and absolute objective changes were 0.0. The relative property and design variable were also unchanged, indicating that the model reached a design minima. However, the maximum constraint of 2.65E-2 exceeded the hard limit of 5.00E-3, which was required for hard convergence.

The decision to accept these results was based on the data presented in Table 1 and Figure 7, which shows the progressions and final values of the objective function, maximum constraint, and individual stress and displacement constraint values. The objective function decreased by ~ 9%, and the engineering values of the displacement and stress were considered acceptable by the design team; therefore, the analysis was stopped and the results were used for design guidance.

Table 1 Optimizer Results

Cycle	Objective	Max Constr	Displ Constr	Stress Const
1	2.756	5.72E-2	5.52E-2	5.72E-2
28	2.511	2.65E-2	2.65E-2	1.97E-2

As with all analytical codes, it is the User's judgment that determines acceptability of the solution. The available information for determining an acceptable optimizer solution includes numerical convergence, predicted engineering results, constraint and objective trends, and shape.

DISCUSSIONS

ANALYSIS

The final optimized shape was evaluated by the entire design team, and the geometry was provided to the stress and thermal engineers, who reperformed the original analyses and verified acceptability. The changes in boundary conditions on the manifold from the original predictions were not considered significant; therefore another optimization analysis was not performed. Had the initial conditions changed appreciably, another optimization pass beginning with the new analyses would have been required.

ELEMENT DISTORTION

One of the primary concerns of shape optimization is the 'distortion' effect of modifying the grid locations while maintaining the same h-element connectivity. Since this was a first attempt at using shape optimization, the relative distortion was monitored, but not used to modify the analysis.

For the original shape, the FE mesh was evaluated using P3's Element Verify capability. The initial mesh had a maximum element Aspect Ratio (AR) of 11, and a maximum edge angle (EA) of 60 degrees. The final mesh (cycle 28) had a maximum AR of 13, and a maximum EA of 67. Although the acceptability of the original mesh may be debated, budgetary constraints and successful correlation with the ongoing stress analysis required that the mesh not be modified. However, it is interesting to note that the maximum characteristics did not change appreciably, despite a significant change in the outer dimensions of the part. In addition, a subsequent detailed stress analysis was performed to verify the distorted elements results.

The intermediate and final shapes were available for viewing by using the grid locations for each design cycle in the .pch file. By copying the punched grid only information into a separate file, then reading the grid file into the P3 model, the existing grids automatically updated to the new modified positions. This procedure was useful for evaluating intermediate results between design cycles and tracking the optimizer's performance. In addition, the Element Verify capability in MSC/P3 could be used to verify element distortion during the run, prior to each design cycle.

It is recommended that the elements always be evaluated after the final cycle, and a final mesh created if any questions on element performance exist. This is a critical reason for bidirectionality of the optimization geometric results with the FE preprocessor, as remeshing without the geometry is difficult and time consuming.

DESIGN IMPACT

This effort proved the value of the optimization process in an integrated design team. Constraints from several areas, including design, manufacturing, and analysis were all incorporated into the final design recommendation. In order to close the loop, however, bidirectionality of the FE optimizer results with the CAD model is also a high priority. In a complicated system, the recommended part shape modification may interfere with associated components. The ability to quickly evaluate several of the intermediate optimizer results in the assembly 3D model would bring the system designer closer to the analysis and allow for a more complete 'system' optimization process, rather than a 'component' based one. In addition, the total design modification time would be reduced, providing the CAE Engineer with more opportunities to contribute to the design.

CONCLUSIONS

The MSC/NASTRAN Shape Optimization capability was successfully used to drive the cast manifold weight down by ~ 9% from the original design, while incorporating input from analysis, manufacturing, and system requirements. The total schedule and budget was significantly less to achieve this modification than if a typical design process of try and see were performed. The addition of

bidirectionality of the shape optimization geometric results with both the CAE preprocessor and the CAD database would significantly enhance the utility of this tool.

ACKNOWLEDGMENTS

Dr. Greg Moore, The MacNeal-Schwendler Corporation
Janie Wallace, Aerojet Propulsion Division

REFERENCES

MSC/NASTRAN Design Sensitivity and Optimization User's Guide, V68

CAST TURBINE MANIFOLD CROSS SECTION MODEL

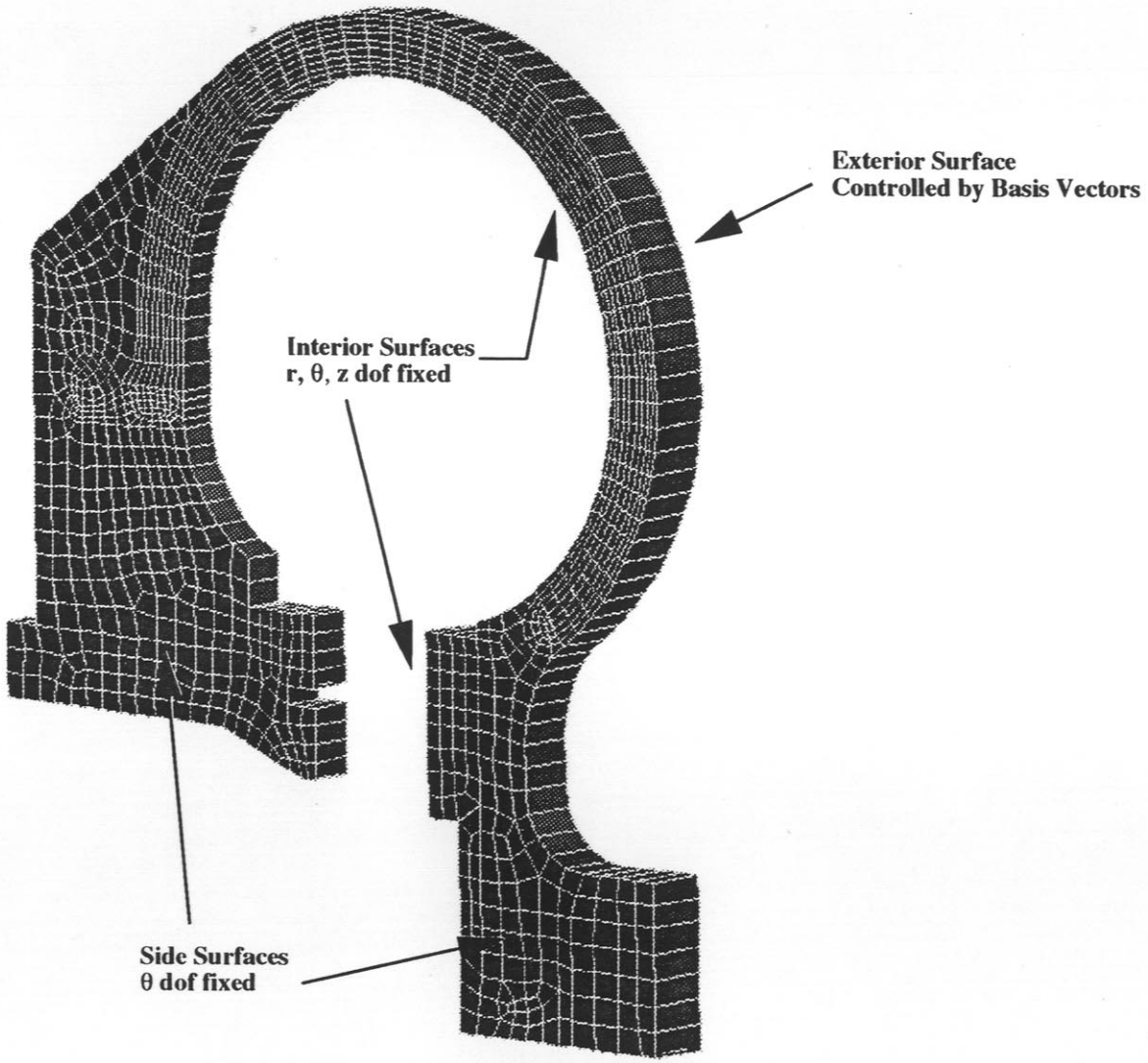

Figure 1

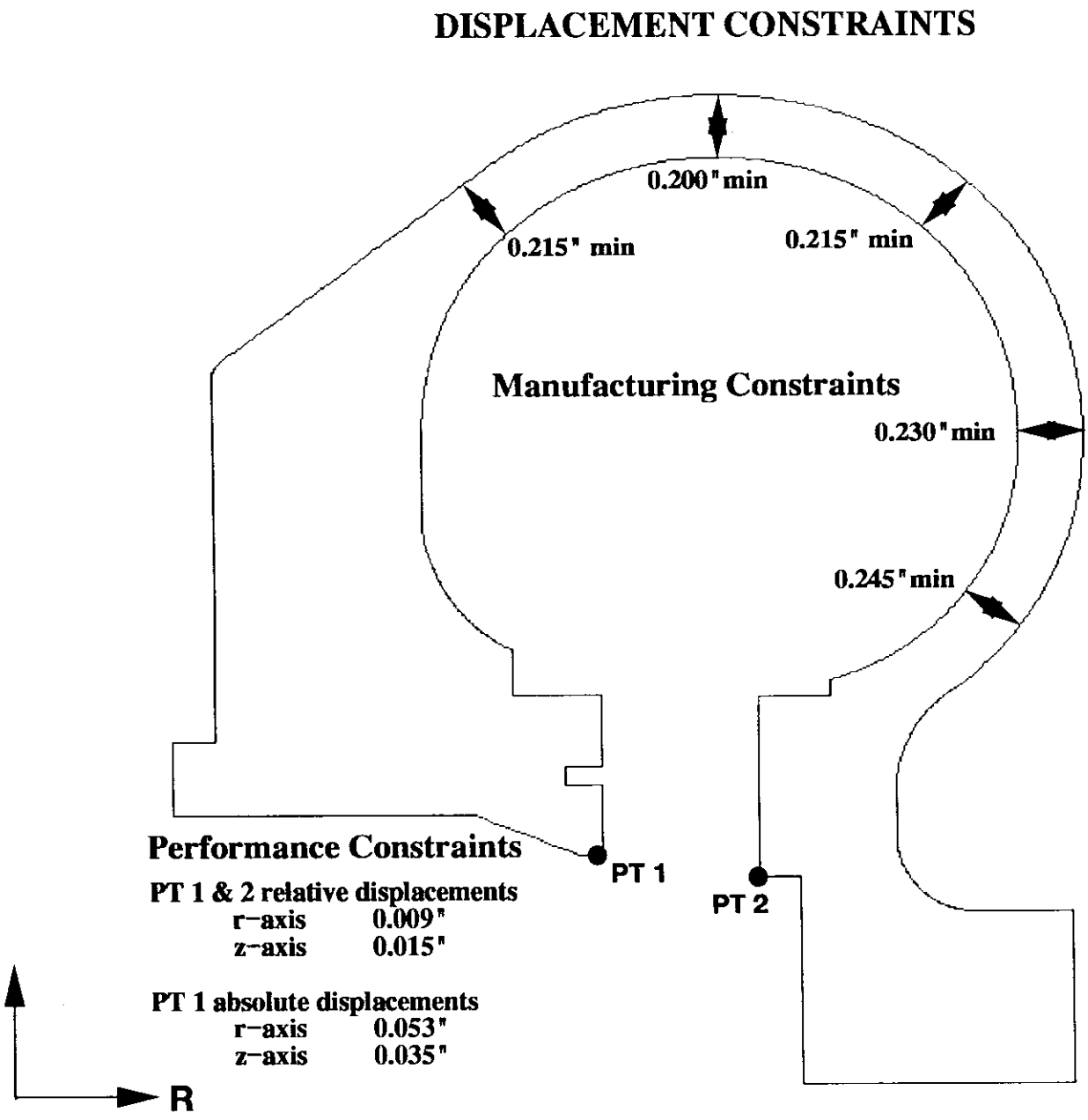
DISPLACEMENT CONSTRAINTS
0.200" min
0.215" min
0.215" min
Manufacturing Constraints
0.230" min
0.245" min
Performance Constraints
PT 1 & 2 relative displacements
r-axis 0.009"
z-axis 0.015"
PT 1 absolute displacements
r-axis 0.053"
z-axis 0.035"
PT 1
PT 2
R

Figure 2

TEMPERATURE DISTRIBUTION

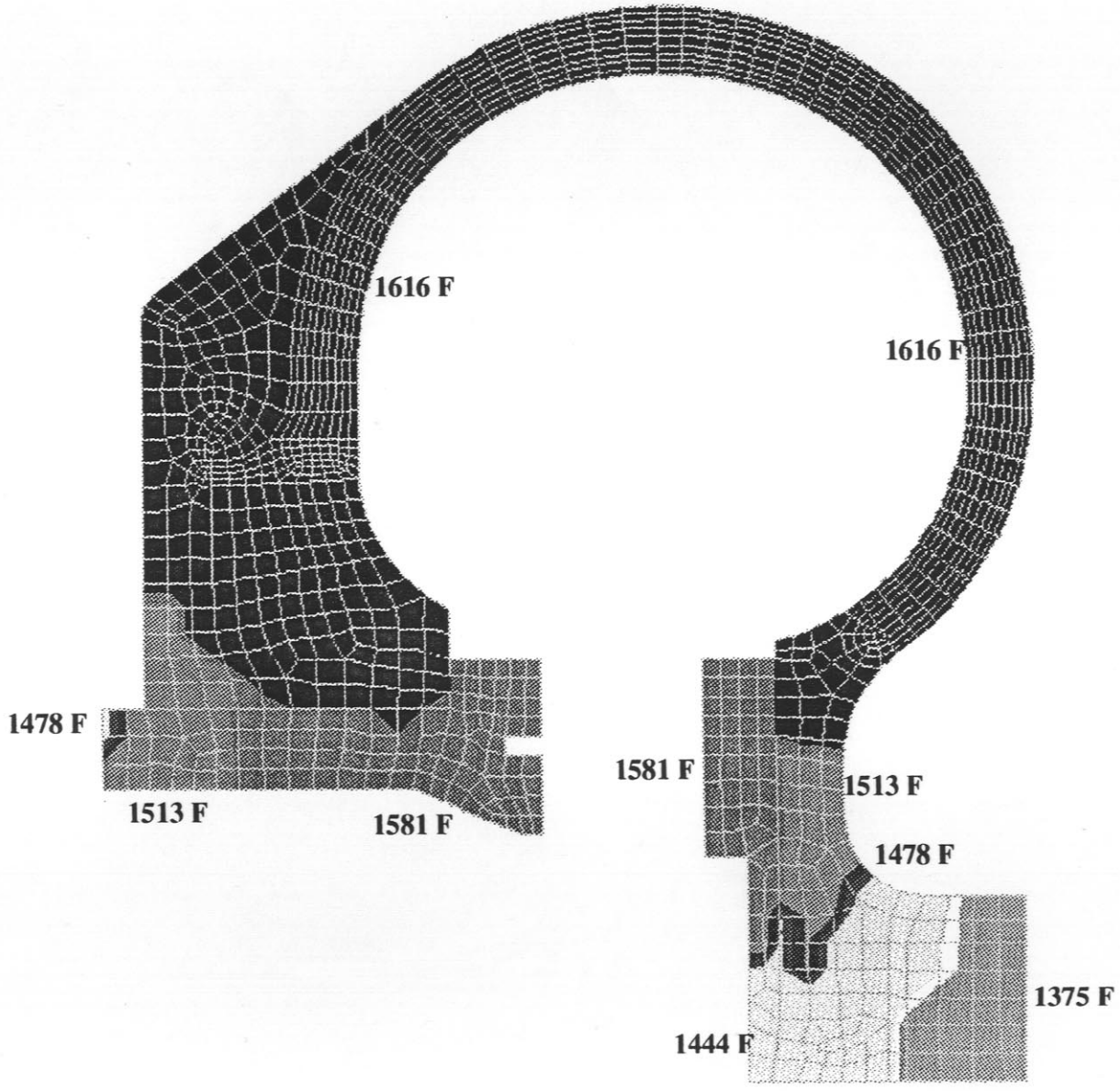

Figure 3

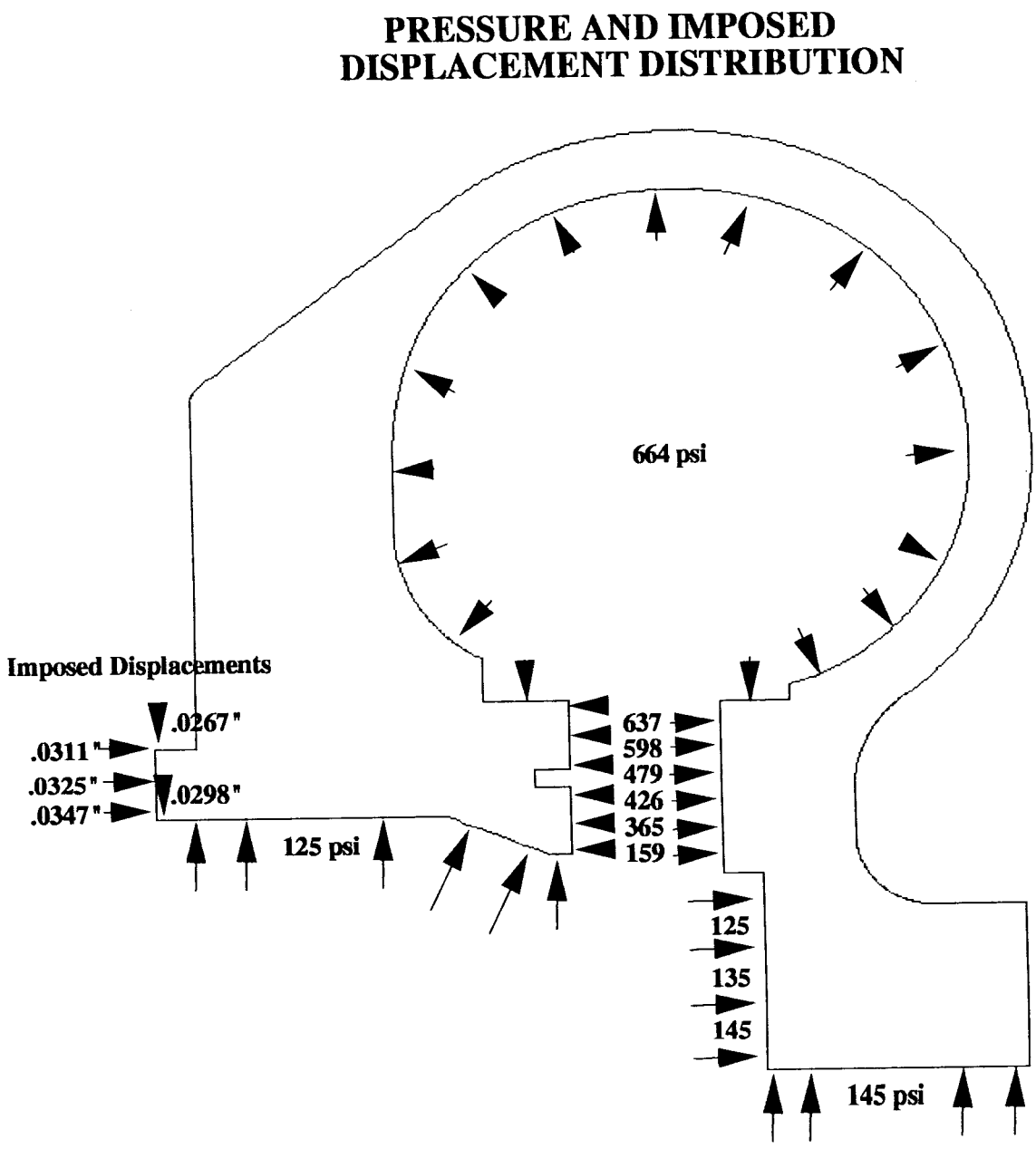
PRESSURE AND IMPOSED
DISPLACEMENT DISTRIBUTION
664 psi
Imposed Displacements
.0267"
.0311"
.0325"
.0347"
.0298"
125 psi
637
598
479
426
365
159
125
135
145
145 psi

Figure 4

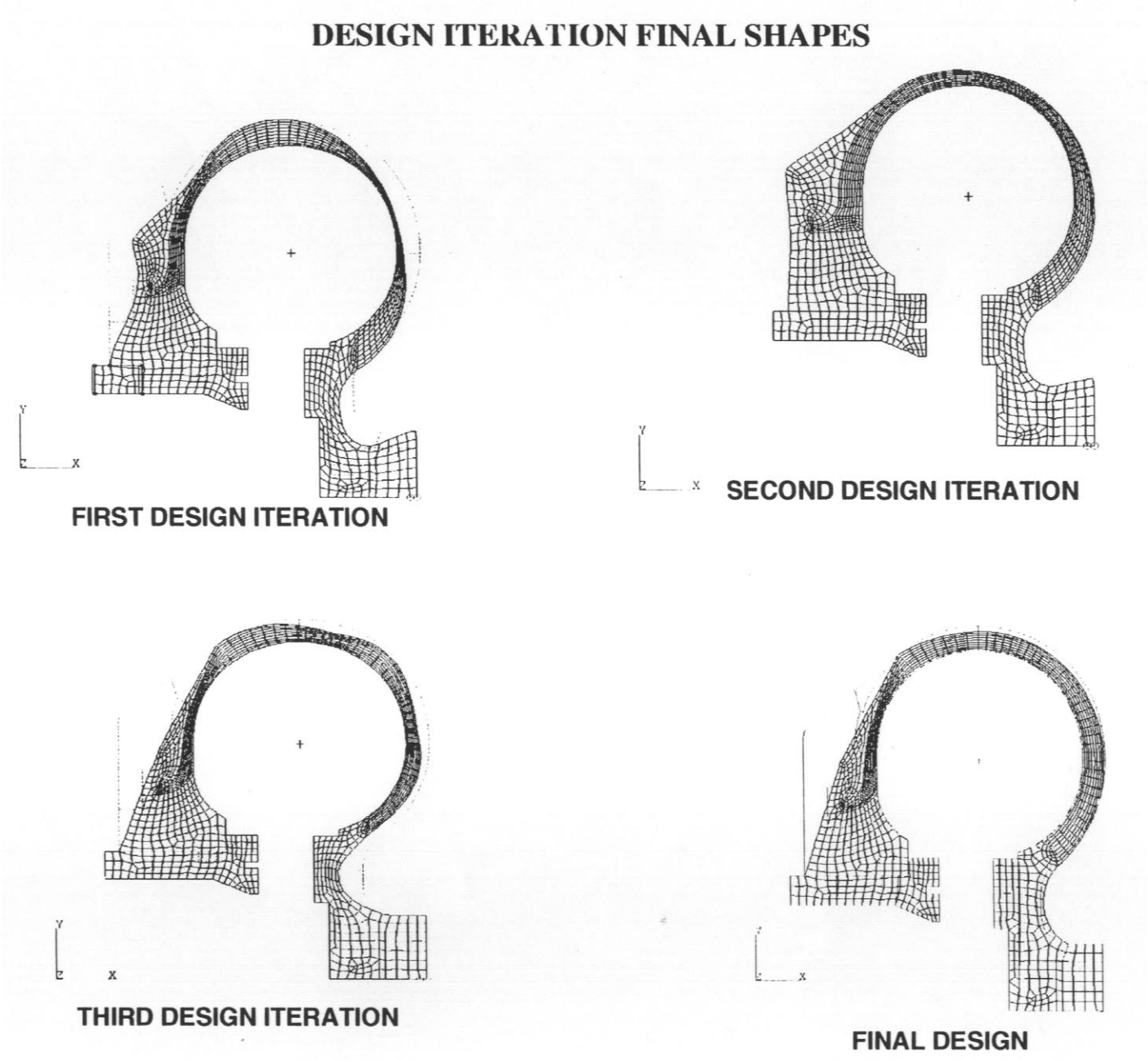
DESIGN ITERATION FINAL SHAPES
FIRST DESIGN ITERATION
SECOND DESIGN ITERATION
THIRD DESIGN ITERATION
FINAL DESIGN

Figure 5

FINAL OPTIMIZATION CYCLE BASIS VECTORS

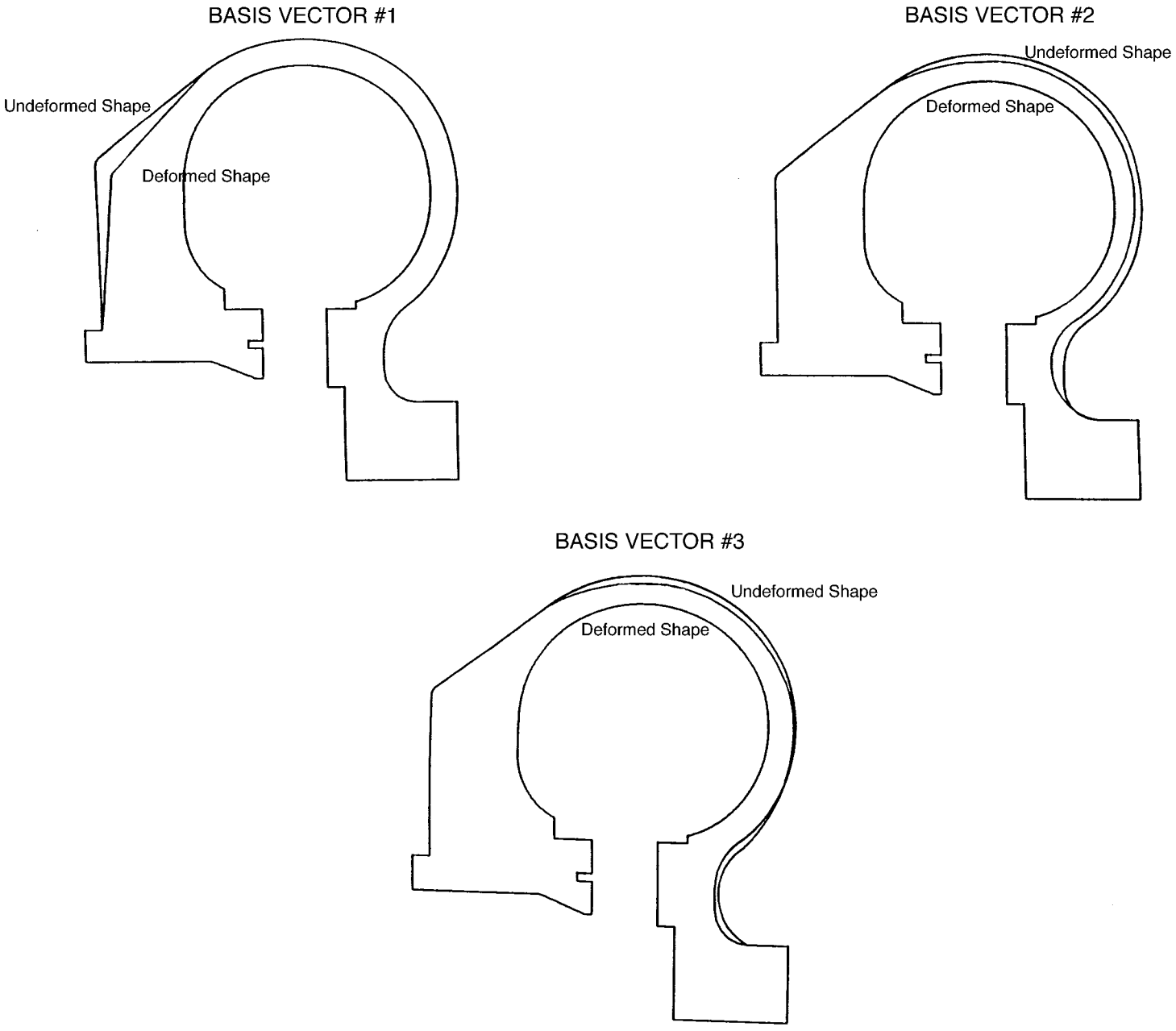

Figure 6

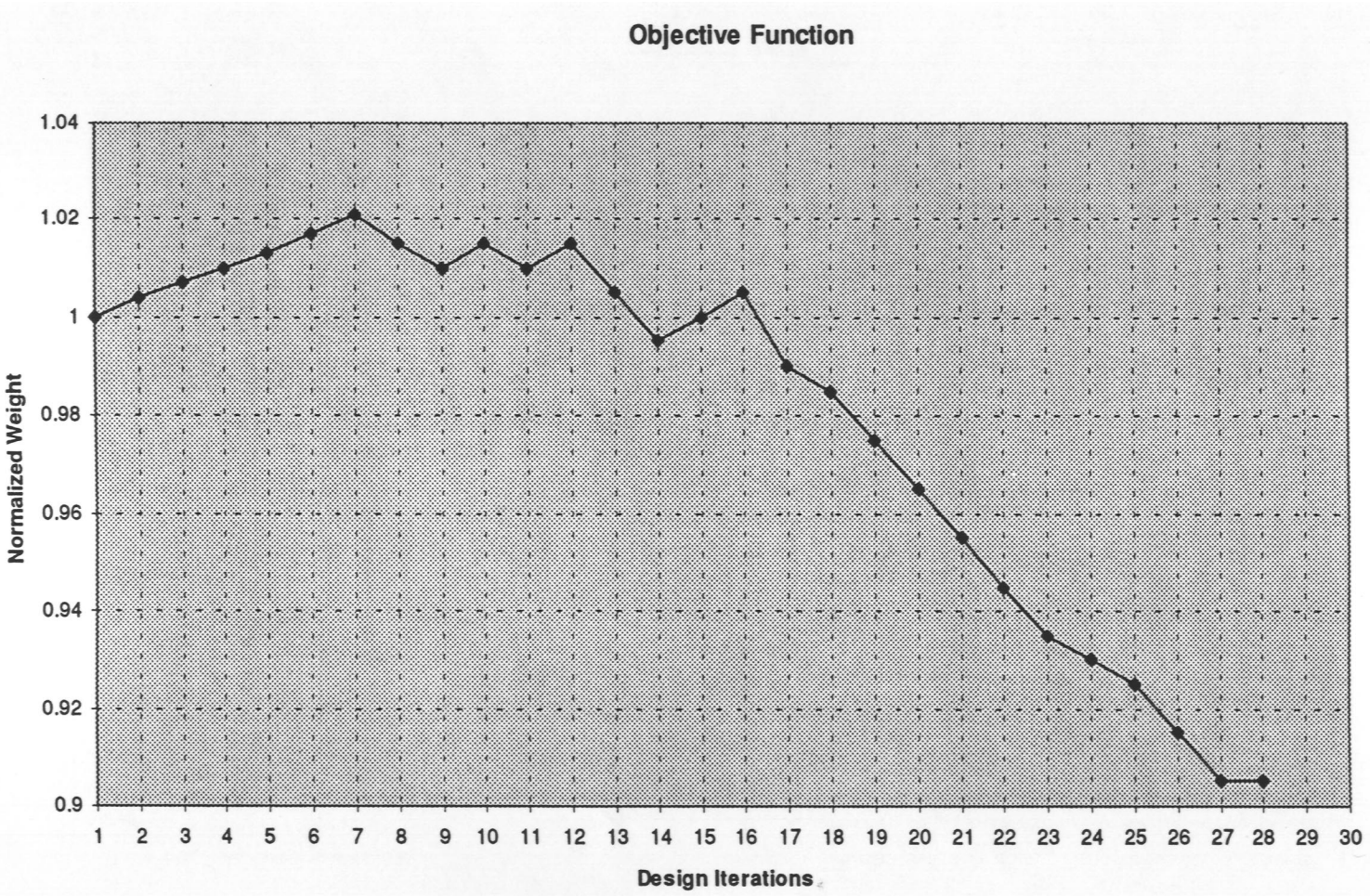
Objective Function
Normalized Weight
1.04
1.02
1
0.98
0.96
0.94
0.92
0.9
1 2 3 4 5 6 7 8 9 10 11 12 13 14 15 16 17 18 19 20 21 22 23 24 25 26 27 28 29 30
Design Iterations

Figure 7